

Density Functional Theory investigation, Hirshfeld surface analysis, Natural bonding orbital study and Docking studies of Triphenylphosphine

K.Rajalakshmi¹ and M.Vetrivel²

¹Department of Physics, SCSVMV, Kanchipuram.

²Department of Mechanical Engineering, SCSVMV, Kanchipuram.

ARTICLE INFO

Article history:

Received: 8 April 2020;

Received in revised form:

30 May 2020;

Accepted: 11 June 2020;

Keywords

Triphenylphosphine,
Density Functional Theory,
Hirshfeld Surface,
NBO,
NLO.

ABSTRACT

Triphenylphosphine [TPP] used in synthesis of organic and organo metallic compounds is investigated for its fundamental reactive properties by density functional theory [DFT] calculations. Natural bond orbital (NBO) analysis enables in comprehending the stability and charge delocalization in the title molecule. Hirshfeld surface analysis for visually analyzing intermolecular interactions in crystal structures employing surface contours and 2D fingerprint plots has been used to scrutinize molecular shapes. Besides NLO, Frontier molecular orbitals and global reactivity descriptors values are calculated. Molecular electrostatic potential map, Fukui Function, Mulliken atomic charges, natural population analysis, Atomic Polar tensors and Thermodynamic analysis were performed. The solvent effects were investigated for obtained molecular energies, hardness and atomic charge distributions were studied for the title compound at TD-DFT method. The binding activity of the molecule with biological targets was examined by docking analysis.

© 2020 Elixir All rights reserved.

1. Introduction

Triphenylphosphine are organo phosphorus compounds containing phosphorus used in pest control as an alternate to chlorinated hydrocarbons. Triphenylphosphine with the formula $C_{18}H_{15}P$ often abbreviated as PPh_3 or Ph_3P widely used in the synthesis of organic and organo metallic compounds. Triphenylphosphine can be prepared in the laboratory by treatment of phosphorus dichloride with phenyl magnesium or phenyl lithium. The industrial synthesis involves the reaction between phosphorus dichloride, chlorobenzene and sodium. [1-3]. Triphenylphosphine crystallizes in triclinic [4] and monoclinic modification [5] and the molecule adopts a pyramidal structure with propeller-like arrangement of the three phenyl groups. It abstracts sulfur from polysulfide compounds, episulfides and elemental sulfur. It is widely used in organic synthesis and its usage are its nucleophilicity and its reducing character [6]. The nucleophilicity of the compound is indicated by its reactivity towards electrophilic alkenes and also used in the synthesis of biaryl compounds.

2. Computational Details

In the present work, the density functional method (DFT) [7] has been employed using Becke's three parameter hybrid exchange functional with the Lee-Yang-Parr correlation functional [8-9] to optimize the structure of the molecule and also to calculate the electronic structure of the title molecule. The entire calculations were performed at ab-initio Hartree Fock (HF) and DFT method using B3LYP levels at 6-31 G (d, p) basis sets on a Pentium V/ 1.6 GHz personal computer using Gaussian 09W program package [10-11] and applying geometry optimization Initial geometry generated was

minimized at the Hartree Fock level using 6-31 G (d, p) basis set.

3. Results and Discussions

The molecule has 34 atoms. A molecule consisting of N atoms has a total of $3N$ degrees of freedom, corresponding to the Cartesian coordinates of each atom in the molecule. In a nonlinear molecule, 3 of these degrees belong to the rotational, 3 of these degrees belong to the translational motions of the molecule and so the remaining corresponds to its vibrational motions. The net number of the vibrational modes is $3N-6$. Therefore, for the title molecule, three Cartesian displacements of 34 atoms provide 96 normal vibration modes. The molecular structure of the molecule is shown in Figure 1.

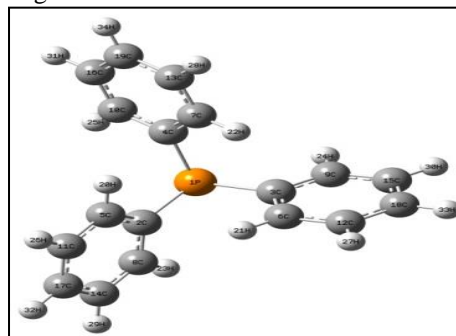


Figure 1. Molecular structure of Triphenylphosphine

3.1 Natural Bonding Orbital analysis

Natural bond orbital (NBO) analysis provides an efficient method for studying intra and intermolecular bonding and interaction among bonds and provides a convenient basis for investigating charge transfer or conjugative interaction in molecular systems. NBO theory also allows the assignment of

the hybridization of atomic lone pairs and of the atoms involved in bond orbitals. Some electron donor orbital, acceptor orbital and the interacting stabilization energy resulted from the second-order micro-disturbance theory are reported. The second-order Fock matrix is carried out to evaluate the donor-acceptor interactions in NBO analysis [12]. The results of interactions are the loss of occupancy from the localized NBO of the idealized Lewis structure into an empty non-Lewis orbital. For each donor (i) and acceptor (j), the stabilization energy $E^{(2)}$ associated with the delocalization $i \rightarrow j$ is estimated as

$$E^{(2)} = E_{ij} = q_i \frac{F(i, j)^2}{(\epsilon_i - \epsilon_j)}$$

where q_i is the donor orbital occupancy, ϵ_i and ϵ_j the diagonal elements and $F(i, j)$ is the off diagonal NBO Fock matrix element. The second order perturbation theory analysis of Fock matrix in NBO shows strong intermolecular hyper conjugative interactions, which are presented in Table 1.

Table 1. Selected natural bond orbital occupancies of the title compound. BD for 2-center bond and BD* for 2-center antibond, a serial number (1, 2, ... if there is a single, double, ... bond between the pair of atoms), and the atom(s) to which the NBO is affixed.

NBO	Occupancies (a.u.)	NBO	Occupancies (a.u.)
BD(1) P1-C2	1.95832	BD*(1)P1-C2	0.03915
BD(1) P1-C3	1.95833	BD*(1)P1-C3	0.03916
BD(1) P1-C4	1.95833	BD*(1)P1-C3	0.03916
BD(1) C2-C5	1.97897	BD*(1)C2-C5	0.02447
BD(2) C2-C5	1.66733	BD*(2)C2-C5	0.36072
BD(2) C3- C6	1.66732	BD*(2)C3-C6	0.36076
BD(1) C4-C7	1.97897	BD*(1)C4-C7	0.02448
BD(1) C5-C11	1.97670	BD*(1)C5-C11	0.01789
BD(1) C5- H20	1.98197	BD*(1)C5-H20	0.01537
BD(1) C6-C12	1.97670	BD*(1)C6-C12	0.01789
BD(1)C6- H21	1.98198	BD*(1)C6-H21	0.01536
BD(1)C7-C13	1.97670	BD*(1)C7-C13	0.01790
BD(1)C8-C14	1.97752	BD*(1)C8-C14	0.01776
BD(2)C8-C14	1.66437	BD*(2)C8-C14	0.31864
BD(1)C8-H23	1.98194	BD*(1)C8-H23	0.01411
BD(1)C9-C15	1.97752	BD*(1)C9-C15	0.01777
BD(1)C9-H24	1.98194	BD*(1)C9-H24	0.01411
BD(1)C10-C16	1.97752	BD*(1)C10-C16	0.01776
BD(1)C10-H25	1.98194	BD*(1)C10-H25	0.01411
BD(1)C11-C17	1.98077	BD*(1)C11-C17	0.01643
BD(2)C11-C17	1.66262	BD*(2)C11-C17	0.32958
BD(1)C11-26	1.98273	BD*(1)C11-H26	0.01230
BD(1)C12-C18	1.98077	BD*(1)C12-C18	0.01644
BD(2)C12-C18	1.66260	BD*(2)C12-C18	0.32959
BD(2) C13-C19	1.66257	BD*(2)C13-C19	0.32960
BD(1)C13-H28	1.98273	BD*(1)C13-H28	0.01230
BD(1)C14-C17	1.98056	BD*(1)C14-C17	0.01646
BD(1)C15-C18	1.98056	BD*(1)C15-C18	0.01646
BD(1)C15-H30	1.98272	BD*(1)C15-H30	0.01212
BD(1)C16-C19	1.98056	BD*(1)C16-C19	0.1646
BD(1)C16-H31	1.98272	BD*(1)C16-H31	0.01212
BD(1)C17-H32	1.98321	BD*(1)C17-H32	0.01210
BD(1)C18-H33	1.98321	BD*(1)C18-H33	0.01211

Table 2. Natural Bond Orbital of Triphenylphosphine.

Donor orbital (i)	Type	Acceptor orbital(i)	Type	E(2)a (Kcal/mol)	E(j)- E(i)b (a.u)	F(i,j)c (a.u)
P1-C2	σ	C5-C11	σ^*	3.33	1.10	0.054
P1-C2	σ	C4-C7	π^*	1.67	0.55	0.029
P1-C2	σ	C8-C14	σ^*	3.81	1.10	0.058
P1-C3	σ	C6-C12	σ^*	3.32	1.10	0.054
P1-C3	σ	C9-C15	σ^*	3.81	1.10	0.058
C2-C5	σ	C2-C8	σ^*	3.54	1.26	0.060
C2-C5	π	C8-C14	π^*	20.04	0.28	0.067
C2-C5	π	C11-C17	π^*	19.49	0.28	0.066
C4-C10	σ	C4-C7	σ^*	3.47	1.26	0.059
C4-C10	σ	C4-H22	σ^*	2.28	1.18	0.046
C4-C10	σ	C10-C16	σ^*	2.84	1.27	0.054
C5-C11	σ	P1-C2	σ^*	3.79	0.86	0.051

C5-C11	σ	C11-C17	σ^*	2.65	1.26	0.052
C5-C11	σ	C11-H26	σ^*	1.31	1.16	0.035
C5-H20	σ	C5-C11	σ^*	0.99	1.09	0.029
C5-H20	σ	C11-H17	σ^*	3.47	1.09	0.055
C7-C13	σ	P1-C4	σ^*	3.79	0.86	0.051
C7-C13	σ	C4-C7	σ^*	3.43	1.25	0.058
C7-C13	σ	C13-C19	σ^*	2.65	1.26	0.052
C8-H23	σ	C2-C5	σ^*	3.61	1.08	0.056
C9-C15	π	C3-C6	π^*	19.57	0.27	0.065
C9-C15	π	C12-C18	π^*	20.71	0.27	0.065
C10-C16	π	C13-C19	π^*	20.72	0.27	0.067
C11-C17	π	C2-C5	π^*	21.55	0.27	0.068
C11-C17	π	C8-C14	π^*	19.99	0.28	0.067
C12-H27	σ	C3-C6	σ^*	3.79	1.08	0.057
C13-H28	σ	C16-C19	σ^*	3.48	1.09	0.029
C14-C17	σ	C8-C14	σ^*	2.71	1.26	0.052
C15-H30	σ	C3-C9	σ^*	3.76	1.058	0.057
C16-H36	σ	C13-C19	σ^*	3.45	1.09	0.055
C17-H32	σ	C5-C11	σ^*	3.53	1.09	0.056
C18-H33	σ	C9-C15	σ^*	3.50	1.10	0.055
C19-H34	σ	C7-C13	σ^*	3.53	1.09	0.056
P1	LP(1)	C2-C5	σ^*	3.18	0.95	0.050
P1	LP(2)	C2-C5	π^*	1.23	0.41	0.022
P1	LP(1)	C3-C6	σ^*	3.18	0.95	0.050
P1	LP(2)	C3-C6	π^*	1.23	0.41	0.022
P1	LP(1)	C4-C7	σ^*	3.18	0.95	0.050
P1	LP(2)	C4-C7	π^*	1.22	0.41	0.022

a $E^{(2)}$ means energy of hyper conjugative interaction (stabilization energy).

b Energy difference between donor and acceptor *i* and *j* NBO orbitals.

c $F(i,j)$ is the Fock matrix element between *i* and *j* NBO orbitals.

The larger the $E^{(2)}$ value, the more intensive is the interaction between electron donors and electron acceptors, i.e. the more donating tendency from electron donors to electron acceptors and the greater the extent of conjugation of the whole system. Delocalization of electron density between occupied Lewis-type (bond or lone pair) NBO orbitals and formally unoccupied (anti-bond or Rydberg) non-Lewis NBO orbitals correspond to a stabilizing donor-acceptor interaction [13-14]. The NBO analysis has been performed to elucidate the intramolecular interaction, rehybridization and delocalization of electron density within the molecule.

The rings with C2,C8,C14,C17,C11,C5 atoms C3,C6,C12,C18,C15,C9 and atoms C4,C7,C10,C13,C16,C19 are typical single-double arrangement attached to P atom at the centre that forms the conjugate structure. The NBO occupancies of single bond of C2-P1,C3-P1 and C4-P1 are of the same level [15].

In the molecule, a strong intramolecular hyper conjugative interaction of π -electrons with the large energy contributions from π (C11-C17) to π^* (C2-C5) have energy value 21.55 kcal/mol. Second large energy contributions from π (C9-C15) to π^* (C13-C19) have energy value 20.72kcal/mol. The same kind of interaction is calculated in π (C2-C5) to π^* (C8-C14) with energy value 20.04 kcal/mol and π (C11-C17) \rightarrow π^* (C8-C14) of energy value 19.99 kcal/mol, π (C2-C5) \rightarrow π^* (C11-C17) and σ (C5-C11) \rightarrow σ^* (P1-C2) with energy value 19.49 and 3.79 kcal/mol,

π (C19-H34) \rightarrow π^* (C7-C13) with energy value 3.53kcal/mol respectively [15-16].

The lone pair interactions were prominent in the title compound as expected due to the charge transfer that taking place from lone pair atom to the atom attached to it. The lone pair contribution from LP(P1) \rightarrow σ^* (C2-C5) σ^* (C3-C6) σ^* (C4-C7) and LP(P1) \rightarrow π^* (C2-C5) π^* (C3-C6) π^* (C4-C7) leads to moderate stabilization of 3.18 kcal/mol and 1.28 kcal/mol respectively.

The results of second order perturbation theory analysis of the Fock matrix and the stabilization energies are presented in Table2. Some strong intramolecular interactions, which are formed by the overlap between σ (C-C), σ^* (C-C) and π (C-C), π^* (C-C) bond orbital in the aromatic ring, which leads intramolecular charge transfer (ICT) causing stabilization of the system have revealed by the NBO analysis. The strong intramolecular hyperconjugative interaction of σ and π electrons of C-C to anti bond C-C of the rings resulting in stabilization of some parts of the rings as evident from Table 2.

The P atom (P1) has negative region and negative molecular electrostatic potential is for the major region of P1 atom. The C8-H23, C10-H25, C9-H24 and C15-30H bonds indicate the major possible site for nucleophilic attack and around of these bonds have maximum positive regions respectively. According to the calculated results, the region of MEP indicates that the negative potential sites are on the electronegative atom and the positive potential sites are around carbon and hydrogen atoms. The determination of

MESP regions is best suitable for identifying sites for inter and intra molecular interactions [17]. According to the MESP surfaces of the compound, the weak negative regions are associated with C11-H26 and C13-H28 atoms and also the weak positive region on the nearby hydrogen atoms.

3.2 Hirshfeld surfaces computational method

The Hirshfeld surfaces and the associated 2D fingerprint plots were calculated using the Crystal Explorer [18] program, which accepts a structure input file in CIF format. A Hirshfeld surface is the outer contour of the space which a molecule or an atom consumes in a crystalline environment. The normalized contact distance d_{norm} based on both d_e (distance from the point to the nearest nucleus external to the surface) and d_i (distance to the nearest nucleus internal to the surface) and the vanderwaals (vdW) radii of the atom, given by the equation given below enables identification of the region of particular importance to intermolecular interactions [19].

The value of the d_{norm} is either negative or positive respectively, shorter or longer vdW separation. Because of the symmetry between d_i and d_e in the expression for d_{norm} , where two Hirshfeld touch, both will display a red spot identical in colour intensity as well as size and shape. The d_{norm} values are mapped onto the Hirshfeld surface using a red-blue-white colour scheme: red regions correspond to closer contacts and negative d_{norm} value, the blue regions correspond to longer contacts and positive d_{norm} and the white regions are those where the distance of contacts is exactly the vdW separation and with a d_{norm} value to zero. The combination of d_e and d_i in the form of 2D fingerprint plot provide summary of intermolecular contacts in the crystal.

$$d_{\text{norm}} = \frac{(d_i - r_i^{\text{vdW}}) - (d_e - r_e^{\text{vdW}})}{r_i^{\text{vdW}} + r_e^{\text{vdW}}}$$

In order to profoundly examine the strength and role of the hydrogen bonds and other intermolecular contacts, and to estimate their importance for the crystal lattice stability, Hirshfeld surface analysis has been conducted. The Hirshfeld surface and 2D fingerprint plots of the title compound is illustrated in Figure 2(a) d_{norm} surface and Figure 2(b). 2D fingerprint plots and the showing surfaces that have been mapped over a d_{norm} range of -0.06 to 1.5 \AA . The surfaces are shown as transparent to allow visualization of the molecular moiety, in a similar orientation for all of the structures. It is seen effectively with the large circular depressions in these spots (deep red) visible on the surfaces indicative of hydrogen-bonding contacts.

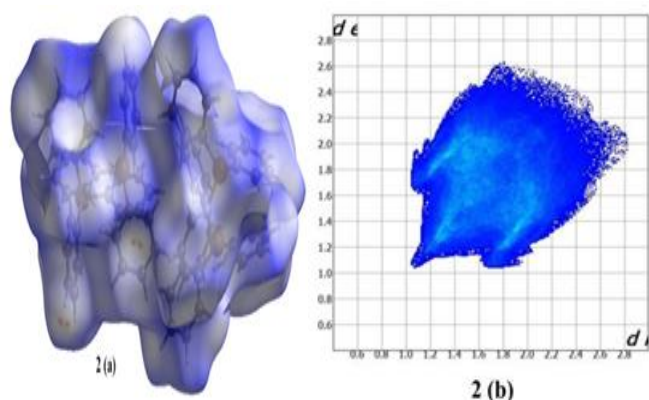


Figure 2. (a) d_{norm} surface (b) 2D Fingerprint plots of Triphenylphosphine

The 2D fingerprint plots, which are used to analyze all of the intermolecular contacts at the same time, revealed that the main intermolecular interactions in the compound were H...H, C...H and H...C. KhaoulaAzouzi et al [20] showing surfaces that have been mapped for shape index and curvature and shown in Figure 3 (a) Hirshfeld surface mapped for curvature Figure 3 (b) shape Index of Triphenylphosphine. Curvature conveys similar information as that of shape index. In fact, the π - π stacking is shown by the pattern of red and blue colors on the same region of the shape index surfaces. It is shown by the large flat region delineated by a blue outline on the curvature surfaces. In order to find out directional interactions, the characteristic features in the fingerprint plots obtained from the Hirshfeld surface were further analyzed.

The Percentage of various intermolecular contacts contributed to the Hirshfeld surfaces present in the title compound is as shown in Figure 4. As previously observed, the highest contribution occurs due to H...H (64.9%) and C...H contacts (16.2%).

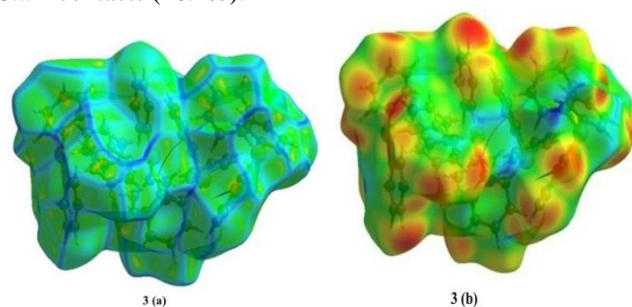


Figure 3. Hirshfeld surface mapped for (a) curvature and (b) shape Index of Triphenylphosphine

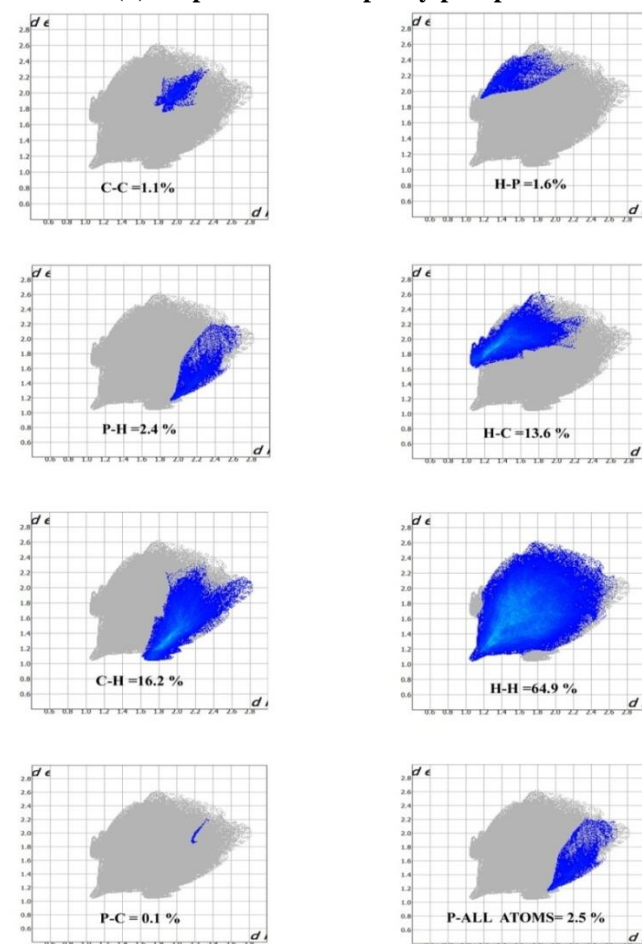


Figure 4. Percentage of various intermolecular contacts contributed to Hirshfeld surfaces.

The C...C interactions are represented by a spike in the bottom left (donor) area of the fingerprint plot, which represents the water oxygen interacting with acid oxygen, forming a 2D network of hydrogen bonds. The H...O interactions are represented by a spike in the bottom right region of fingerprint plot (acceptor). The proportion of H...H interactions comprises 64.9% of the of the total Hirshfeld surfaces. Lower percentages are observed for the P...H(2.4%) /P...C (0.1%) and C...C (1.1%) contacts, with the last contact contribution corresponding largely to other interactions. The relative contribution of the different interactions to the Hirshfeld surface is H...H/C...H interactions have major participations in crystal structures.

3.3 Molecular Electrostatic Potential (MESP)

To investigate reactive sites for electrophilic and nucleophilic attack, the regions of the MEP for the title compound was composed at DFT calculation using the optimized geometry at the B3LYP/6-31G(d, p). As shown in Figure 5, red and yellow colors indicate negative regions in MEP corresponding to electrophilic reactivity, while bluish green colors indicate for positive regions corresponding to nucleophilic reactivity. So, the compound has one major possible site for electrophilic attack.

The P atom (P1) has negative region and negative molecular electrostatic potential is for the major region of P1 atom. The C8-H23, C10-H25, C9-H24 and C15-30H bonds indicate the major possible site for nucleophilic attack and around of these bonds have maximum positive regions respectively. According to the calculated results, the region of MEP indicates that the negative potential sites are on the electronegative atom and the positive potential sites are around carbon and hydrogen atoms. The determination of MESP regions is best suitable for identifying sites for inter and intra molecular interactions [21]. According to the MESP surfaces of the compound, the weak negative regions are associated with C11-H26 and C13-H28 atoms and also the weak positive region on the nearby hydrogen atoms.

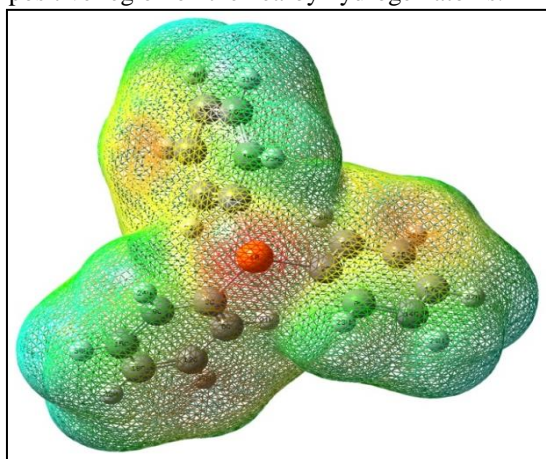


Figure 5. MESP of Triphenylphosphine

3.4 Frontier Molecular Orbitals

To provide a reasonable qualitative indication of the excitation properties, the highest occupied molecular orbital (HOMO) and the lowest unoccupied molecular orbital (LUMO) for the title compound were investigated. The frontier molecular orbital distributions and energy levels of the HOMO, LUMO, HOMO-1, and LUMO+1 and HOMO-2, and LUMO+2 were computed at B3LYP/6-31 G(d) level of the title compound [21]. Both the highest occupied molecular orbitals (HOMOs) and the lowest-lying unoccupied molecular orbitals (LUMOs) are mostly the π -anti bonding type

molecular orbitals in the structure. The frontier molecular orbital shows π molecular orbital characteristics and are visualized in Figure 6 and Density of States (DOS) spectrum is shown in Figure 7. The HOMO and LUMO are mainly localized on the whole structure, The HOMO-2 is localized on entire ring containing C3 and C4 atoms and partly on ring of C2 except P atom, whereas LUMO+2 is localized on the entire structure and partly on P atom.

Global Reactivity Descriptors and Electronic Properties:

The ionization potential (IP) and electron affinity (EA) are determined from the energy difference between the (3) energy of the compound derived from electron transfer which is approximated as; IP -E and EA HOMO -ELUMO respectively based on Koopman's theorem [21]. The chemical hardness (η), chemical potential (μ), softness ($1/2 \eta$) and electrophilicity index (ω) of a molecule are deduced from IP and EA values [22-25].

The electrophilicity index has been used as structural depictor for the analysis of the chemical reactivity of molecules [26-28]. It measures the propensity of a species to accept electrons. A good, more reactive, nucleophile is characterized by a lower value of μ, ω and in opposite a good electrophile is characterized by a high value of μ, ω . The electro negativity and hardness are used extensively to predict the chemical behavior to explain aromaticity in organic compounds [25]. A hard molecule has a large HOMO-LUMO gap and a soft molecule has a small HOMO-LUMO. The LUMO represents electron(s) accepting ability and HOMO as electron donating ability of a molecule.

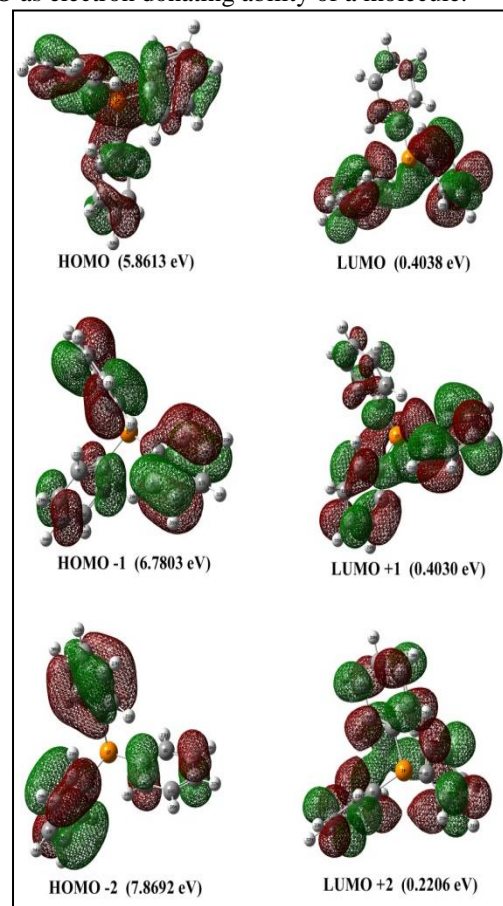


Figure 6. Frontier Molecular orbitals of Triphenylphosphine.

The chemical hardness is useful to rationalize the relative stability and reactivity of chemical compounds. There are large HOMO-LUMO gap in the hard compounds and more stable and less reactive than soft compounds having small HOMO-LUMO gap. The definitions of universal concepts of

molecular structure stability and reactivity can be provided by using DFT method and from the definition of hardness η , the following equation of hardness is developed. In the expression given below I is the vertical ionization energy and A stands for the vertical electron affinity. According to Koopman theorem, [25] the ionization energy and electron affinity can be equalized through HOMO and LUMO orbital energies $EA = -E_{\text{HOMO}}$, $IP = -E_{\text{LUMO}}$. The hardness corresponds to the gap between the HOMO and LUMO orbitals. Hence, the larger the HOMO-LUMO energy gaps the harder the molecule.

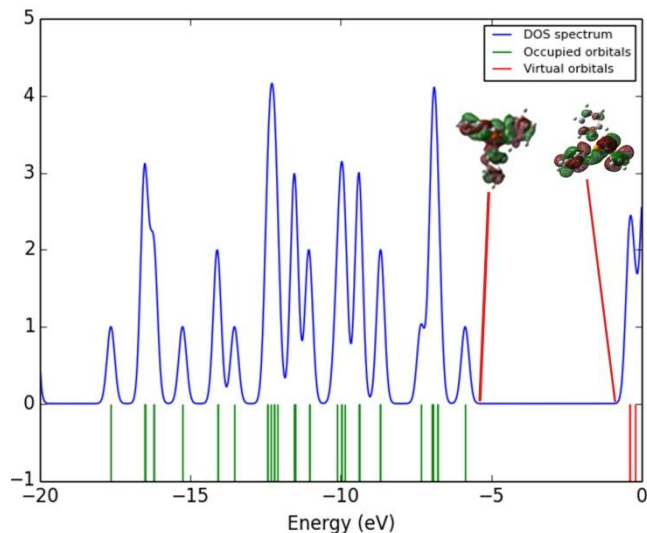


Figure 7. DOS spectrum of Triphenylphosphine

For the title compound, chemical hardness (η) were calculated with the B3LYP/6-31G(d) level. The results are given in Table 3. The energy separation between the HOMO and LUMO is 5.45752 eV and this large HOMO-LUMO gap suggests that high excitation energies for many of excited states, a good stability and high chemical hardness for the title compound. Indeed as seen from Table 3, the chemical hardness of the compound ($\eta = 2.72876$ eV) is smaller than observed in other solvents and higher in DMSO ($\eta = 2.76889$ eV), which indicates hardness and stability increases in solvents.

3.5 Atomic Charge Distributions in Gas-Phase and in Solution-Phase

Mulliken atomic charges for non-H atoms of the compound were calculated at B3LYP/6-31G(d, p) level in gas-phase. In order to investigate the solvent effect selected three kinds of solvent ($\epsilon = 4.9$, chloroform; $\epsilon = 46.7$, DMSO; $\epsilon = 24.55$, ethanol;), the atomic charge distributions were also calculated at B3LYP/6-31G(d) level [26-28]. The calculated values of atomic charges of the title compound in gas-phase and solution-phase listed as shown in Table 4. According to the calculated Mulliken atomic charges, the P1 atom have bigger positive atomic charges in gas-phase than in solution phase. On the other hand, the atomic charge values in solution-phase increases than those in gas-phase and while their atomic charges are becoming more negative with the increase of the polarity of the solvent.

Table 4. Atomic charges of Triphenylphosphine in gas-phase and solution-phase.

Atom	In gas-phase ($\epsilon=1$) B3LYP/ 6-31 G(d,p)	In solution-phase B3LYP/6-31 G(d,p)		
		Chloroform ($\epsilon=4.9$)	DMSO ($\epsilon=46.7$)	Ethanol ($\epsilon=24.55$)
P1	0.618076	0.600104	0.588359	0.58728
C2	-0.269863	-0.239773	-0.239514	-0.239529
C3	-0.269602	-0.239707	-0.239427	-0.239445
C4	-0.284979	-0.239834	-0.239529	-0.239554
C5	-0.113051	-0.147668	-0.149339	-0.149160
C6	-0.126552	-0.147833	-0.149439	-0.149271
C7	-0.108961	-0.147746	-0.149417	-0.149238
C8	-0.127441	-0.147910	-0.152465	-0.151929
C9	-0.120969	-0.147830	-0.152417	-0.151876
C10	-0.121527	-0.147900	-0.152473	-0.151936
C11	-0.117546	-0.122141	-0.129501	-0.125492
C12	-0.119866	-0.122104	-0.125905	-0.125489
C13	-0.123197	-0.122127	-0.125877	-0.125469
C14	-0.117963	-0.121405	-0.125367	-0.124927
C15	-0.119296	-0.121404	-0.125341	-0.124906
C16	-0.120327	-0.121440	-0.125365	-0.124933
C17	-0.127095	-0.140459	-0.144238	-0.143823
C18	-0.127508	-0.140467	-0.144277	-0.143858
C19	-0.124701	-0.140566	-0.144312	-0.143903

3.6 Nonlinear Optical Properties(NLO)

Non-linear optical (NLO) effects arise from the interactions of electromagnetic fields in various media to produce new fields altered in phase, frequency, amplitude or other propagation characteristics from the incident fields [29]. For an isolated molecule, the nonlinear optical response in an electric field $E_i(\omega)$ can be presented as a Taylor series expansion of the total

$$\mu_{\text{tot}} = \mu_0 + \alpha_{ij}E_j + \beta_{ijk}E_jE_k + \dots$$

Where α_{ij} is the linear polarizability, μ_0 the permanent dipole moment and β_{ijk} are the first hyperpolarizability tensor components. The isotropic (or average) linear polarizability is defined as [30]

$$\alpha_{\text{tot}} = (\alpha_{xx} + \alpha_{yy} + \alpha_{zz}) / 3$$

First hyperpolarizability is a third rank tensor that can be described by $3 \times 3 \times 3$ matrix. The 27 components of 3D matrix can be reduced to 10 components due to the Kleinman symmetry [31]. The output from Gaussian 09 provides 10 components of this matrix as β_{xxx} , β_{xxy} , β_{xyy} , β_{yyy} , β_{xxz} , β_{xyz} , β_{yyz} , β_{xzz} , β_{yzz} , β_{zzz} , respectively. The components of the first hyperpolarizability can be calculated using the following equation [32]:

$$\beta_i = \beta_{iii} + 1/3 \sum (\beta_{ijj} + \beta_{jij} + \beta_{jji})$$

Using the x, y and z components of β , the magnitude of the first hyperpolarizability tensor can be calculated by:

$$\beta_{\text{tot}} = (\beta_x^2 + \beta_y^2 + \beta_z^2)^{1/2}$$

Table 3. Calculated total energies, Hardness and frontier orbital energies of Triphenylphosphine.

Energy	Gas phase (eV)	Chloroform (eV)	DMSO (eV)	Ethanol (eV)
$E_{\text{Total}}[\text{Hartree}]$	-1036.11018	-1036.114	-1036.1166	-1036.116
E_{HOMO}	-5.86133	-6.01861	-6.09861	-6.08936
E_{LUMO}	-0.40381	-0.50613	-0.56082	-0.55429
$E_{\text{HOMO}} - E_{\text{LUMO}}$	5.45752	5.51248	5.53779	5.53507
Chemical hardness (η)	2.72876	2.75624	2.76889	2.76753
Chemical potential (μ)	-2.72876	-2.75624	-2.76889	-2.76753
Softness (S)	0.18323	0.18140	0.18057	0.18066
Electrophilicity index (ω)	1.36438	1.37812	1.39445	1.38376

The complete equation for calculating the magnitude of β from Gaussian 09 output is given as follows:

$$\beta_{\text{tot}} = \sqrt{(\beta_{xxx} + \beta_{xyy} + \beta_{xzz})^2 + (\beta_{yyy} + \beta_{yzz} + \beta_{yxx})^2 + (\beta_{zzz} + \beta_{zxx} + \beta_{zyy})^2}$$

Table 5. The dipole moments μ (D), polarizability α , the average polarizability α (esu), the anisotropy of the polarizability $\Delta\alpha$ (esu), and the first hyperpolarizability β (esu) of Triphenylphosphine calculated at B3LYP/6-31G(d,p) method.

PARAMETERS	DFT/B3LYP/6-31G(d,p)
β_{xxx}	84.7684
β_{xyy}	-18.6948
β_{xvv}	81.0344
β_{yyv}	23.7559
β_{xxx}	-49.1804
β_{xvz}	1.9889
β_{vzz}	-50.7022
β_{xzz}	1.8881
β_{vzz}	-2.8528
β_{zzz}	19.3203
$\beta_{\text{tot}}(\text{esu}) \times 10^{-33}$	1.6073×10^{-30} esu
μ_x	0.0090
μ_y	0.01351
μ_z	-0.5887
$\mu_{\text{tot}}(\text{D})$	0.6455
α_{xx}	219.5647
α_{yy}	0.01991
α_{zz}	219.6053
α_{xy}	-0.8878
α_{xz}	1.3757
α_{yz}	161.7343
$\alpha(\text{esu}) \times 10^{-24}$	146.3966
$\Delta\alpha(\text{esu}) \times 10^{-24}$	2.16959

DFT has been extensively used as an effective method to investigate the organic NLO materials [32]. The electronic dipole moment μ_i ($i = x, y, z$), polarizability α_{ij} and the first hyperpolarizability β_{ijk} of the title compound were calculated at the B3LYP/6-31G(d,p) level and listed in Table 5.

Since the values of the polarizability ($\Delta\alpha$) and the hyperpolarizability (β_{tot}) of the GAUSSIAN 09 output are obtained in atomic units (a.u.), the calculated values have been converted into electrostatic units (esu.) (for α ; 1 a.u. = 0.1482×10^{-24} esu., for β ; 1 a.u. = 8.6393×10^{-33} esu.). The calculated values of dipole moment (μ) for the title compounds were found to be 0.0090, 0.0135, -0.5887 and 0.6455D respectively. Urea is one of the prototypical molecules used in the study of the NLO properties of molecular systems. Therefore, it has been used frequently as a threshold value for comparative purposes. The calculated values of polarizability is 146.3966×10^{-24} and the value of anisotropy of polarizability are 2.16959 esu, respectively. The magnitude of the molecular hyperpolarizability (β) is one of important key factors in a NLO system. The calculated first hyperpolarizability value (β) of the title molecule is equal to 1.6073×10^{-30} esu. The above results show that the title molecule is found to be suitable for NLO applications.

3.7 Molecular Docking

Molecular docking has recently been used as a convenient tool to obtain insights into the molecular mechanism of protein-ligand interactions. Molecular docking studies were carried out to evaluate the binding affinity of the ligand with the active site

of mmdb_6KBW[33]. The title molecule was chosen to be docked into the active site of receptors mmdb_6KBW obtained from Protein Data Bank (PDB). The docking calculations were carried out using the AutoDockVina software and as reported in the literature [34]. The protein-ligand interaction with and for visualization performed using PYMOL [35-36]. The ligand was docked into the functional sites of the respective proteins individually and the docking energy was examined to achieve a minimum value. The docked conformation which had the lowest binding energy was chosen to investigate the mode of binding. the results have been shown in Table 6. The docking protocol predicted the same conformation as was present in the crystal structure with RMSD value well within the reliable range of 2 Å. The ligand binds at the active site of the substrate by weak non-covalent interactions and these interactions are depicted in Figure 8. According to the obtained results it was concluded that the docked ligands form a stable complex with nine representative binding modes have been detected with binding affinities ranging from -6.9 kcal/mol to -6.3 kcal/mol. It is clear that the most effective Binding free energy of -6.9 kcal/mol as predicted by Auto Dock Vina suggests good binding affinity.

Table 6. Results of Docked conformation of Triphenylphosphine.

Ligand	PDB ID	Binding affinity	Mode	RMSD Lower band	RMSD Higher band
Title compound	6BKW	-6.9	0	0.0	0.0
		-6.9	1	0.107	5.304
		-6.8	2	0.07	5.285
		-6.5	3	6.203	8.947
		-6.5	4	1.373	4.535
		-6.4	5	6.287	8.937
		-6.4	6	3.684	6.906
		-6.3	7	3.672	6.918
		-6.3	8	3.634	6.785

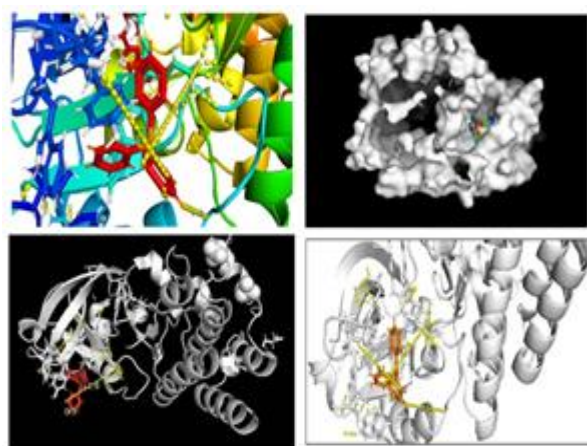


Figure 8. Docking of Triphenylphosphine.

3.8 Mulliken population analysis (MPA) and natural population analysis (NPA)

The calculated MPA NPA and Atomic Polar tensors (APT) are listed in Table 7. The better represented graphical forms of the results were depicted in Figure 9.

Atom Numbering	Atom	MPA	NPA	APT
1	P	0.618076	0.625173	0.554274
2	C	-0.269863	-0.240987	-0.105529
3	C	-0.269602	-0.240927	-0.105388
4	C	-0.284979	-0.240983	-0.105627
5	C	-0.113051	-0.143480	-0.107867
6	C	-0.126552	-0.143685	-0.107905
7	C	-0.108961	-0.143562	-0.17819
8	C	-0.127441	-0.138580	-0.058031
9	C	-0.120969	-0.138520	-0.058122
10	C	-0.121527	-0.138508	-0.058030
11	C	-0.117546	-0.112493	-0.008402
12	C	-0.119866	-0.112470	-0.008401
13	C	-0.123197	-0.112433	-0.008508
14	C	-0.117983	-0.111671	-0.008517
15	C	-0.119296	-0.111647	-0.008517
16	C	-0.120327	-0.111637	-0.008526
17	C	-0.127095	-0.130952	-0.023025
18	C	-0.127508	-0.130955	-0.023033
19	C	-0.124701	-0.130990	-0.022963
20	H	0.151885	0.147855	0.051815
21	H	0.151077	0.147853	0.051639
22	H	0.156386	0.147866	0.051590
23	H	0.142064	0.138932	0.045473
24	H	0.140558	0.138938	0.045511
25	H	0.140761	0.138927	0.045454
26	H	0.127311	0.127261	0.007813
27	H	0.125043	0.127262	0.007800
28	H	0.126527	0.127276	0.007818
29	H	0.128690	0.127878	0.007448
30	H	0.126734	0.127883	0.007454
31	H	0.127488	0.127884	0.007458
32	H	0.127191	0.127821	0.014212
33	H	0.124489	0.127833	0.014230
34	H	0.126183	0.127837	0.014222

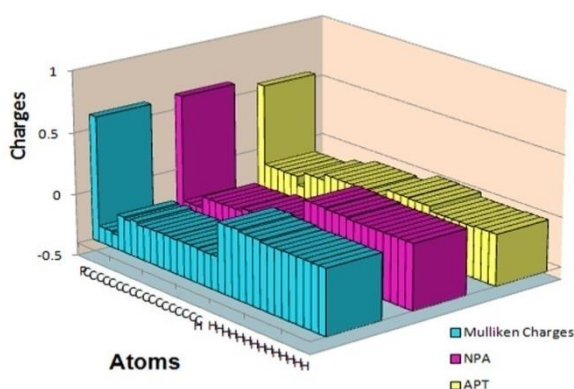


Figure 9. MPA,NPA and APT analysis of Triphenylphosphine

The magnitude of carbon atomic charges is found to be negative, The magnitude of hydrogen atomic charges is found to be positive and is the order from 0.007448 to 0.156386 for the title compound. The maximum atomic charges is obtained for P1 attached at the centre of the three rings having negatively charged carbon atoms [37].

3.9 Fukui Function

Fukui indices are in short, reactivity indices they give us information regarding the tendency of the molecule tendency to either loose or accept electrons so that they tend to do

nucleophilic or electrophilic attack respectively. The Fukui function is defined as [38]

$$f = \left(\frac{\delta(r)}{\delta(N)} \right)_r$$

where $\delta(r)$ is that the electronic density, N is the number of electrons and r is the external potential exerted. Fukui Function (FF) is one of the useful local density functional descriptors to model chemical reactivity, The Fukui Function may be a local reactivity descriptor that indicates the number of electron modified. Therefore, it indicates the propensity of the electron density to perform at a given position upon accepting or donating electrons [39]. Also, it is possible to define the corresponding condensed or atomic Fukui Functions on the j^{th} atom site as,

$$f_j^+ = q_j(N+1) - q_j(N)$$

$$f_j^- = q_j(N) - q_j(N-1)$$

$$f_j^0 = \frac{1}{2} [q_j(N+1) - q_j(N-1)]$$

where f_j^+ , f_j^- , f_j^0 are nucleophilic, electrophilic and free radical on the reference molecule respectively. In these equations, q_j is that the atomic charge (evaluated from Mulliken population, electrostatic derived charge, etc) at the j^{th} atomic site is the neutral (N), anionic (N+1) or (n-1) chemical species. Chattaraj et al. [40] have introduced the thought of generalized philicity. It contains the majority

information concerning hitherto well known completely different global and local reactivity and selectivity descriptor, in additionally to the data concerning electrophilic/nucleophilic power of a given atomic site for the molecule. Morell et.al [41] has recently planned a dual descriptor ($\Delta f(r)$), which is defined as the difference between the nucleophilic and electrophilic Fukui function and is given by the equation,

$$\Delta f(r) = [f_j^+(r) - f_j^-(r)]$$

$\Delta f(r) > 0$, then the site is favoured for a nucleophilic attack, whereas $\Delta f(r) < 0$, r then the site is favored for an electrophilic attack.

According to dual descriptor $\Delta f(r)$ give a transparent distinction between nucleophilic and electrophilic attack at a particular site with their sign. That is they provide a positive value prone for electrophilic attack. From the values reported in Table 8, according to the condition for dual descriptor, nucleophilic site in out title molecule is P1,C5,C6,C7,C8,C9,C10, C12, C14,C15,C16, C17,C18,C19, and H20 to H34 have Positive values i.e. $\Delta f(r) > 0$. Similarly the electrophilic site is C2, C3,C4,C11 and C13 have Negative values i.e. $\Delta f(r) < 0$. The behaviour of the molecule as nucleophilic and electrophilic attack throughout reaction depends on the local behavior the molecule.

Table 8. Mulliken population analysis: Fukui functions (f_j^+, f_j^-, f_j^0) for Triphenylphosphine.

Atom	Mulliken atomic charges			Fukui functions			$\Delta f(r)$
	$q_i(N+1)$	$q_i(N_0)$	$q_i(N-1)$	f_j^+	f_j^-	f_j^0	
P1	0.808105	0.383933	0.393231	0.424172	-0.009298	0.414874	0.43347
C2	-0.274008	-0.200049	-0.217934	-0.073959	0.017885	-0.056074	-0.09184
C3	-0.274009	-0.200059	-0.202699	-0.07395	0.00264	-0.07131	-0.07659
C4	-0.274009	-0.200044	-0.214939	-0.073965	0.014895	-0.05907	-0.08886
C5	-0.065050	-0.107882	-0.097074	0.042832	-0.010808	0.032024	0.05364
C6	-0.065050	-0.107868	-0.114675	0.042818	0.006807	0.049625	0.036011
C7	-0.065050	-0.107877	-0.101205	0.042827	-0.006672	0.036155	0.049499
C8	-0.067222	-0.100615	-0.080235	0.033393	-0.02038	0.013013	0.053773
C9	-0.067222	-0.100606	-0.093802	0.033384	-0.006804	0.02658	0.040188
C10	-0.067222	-0.100627	-0.081591	0.033405	-0.019036	0.014369	0.052441
C11	-0.156401	-0.166170	-0.177857	0.009769	0.011687	0.021456	-0.00192
C12	-0.156401	-0.166178	-0.167828	0.009777	0.00165	0.011427	0.008127
C13	-0.156401	-0.166167	-0.178244	0.009766	0.012077	0.021843	-0.00231
C14	-0.156191	-0.167940	-0.177867	0.011749	0.009927	0.021676	0.001822
C15	-0.156191	-0.167949	-0.167525	0.011758	-0.000424	0.011334	0.012182
C16	-0.156191	-0.167938	-0.176404	0.011747	0.008466	0.020213	0.003281
C17	-0.055700	-0.125960	-0.114791	0.07026	-0.011169	0.059091	0.081429
C18	-0.055699	-0.125951	-0.127595	0.070252	0.001644	0.071896	0.068608
C19	-0.055700	-0.125962	-0.116652	0.070262	-0.00931	0.060952	0.079572
H20	0.159970	0.153735	0.151452	0.006235	0.002283	0.008518	0.003952
H21	0.159970	0.153734	0.152877	0.006236	0.000857	0.007093	0.005379
H22	0.159970	0.153734	0.153854	0.006236	-0.00012	0.006116	0.006356
H23	0.159422	0.150473	0.148977	0.008949	0.001496	0.010445	0.007453
H24	0.159422	0.150473	0.150141	0.008949	0.000332	0.009281	0.008617
H25	0.159422	0.150473	0.148869	0.008949	0.001604	0.010553	0.007345
H26	0.175072	0.146578	0.147624	0.028494	-0.001046	0.027448	0.02954
H27	0.175072	0.146579	0.145778	0.028493	0.000801	0.029294	0.027692
H28	0.175072	0.146578	0.147025	0.028494	-0.000447	0.028047	0.028941
H29	0.175094	0.146905	0.148549	0.028189	-0.001644	0.026545	0.029833
H30	0.175094	0.146906	0.146937	0.028188	-0.000031	0.028157	0.028219
H31	0.175094	0.146905	0.147848	0.028189	-0.000943	0.027246	0.029132
H32	0.168981	0.142945	0.141967	0.026036	0.000978	0.027014	0.025058
H33	0.168981	0.142945	0.142125	0.026036	0.00082	0.026856	0.025216
H34	0.168981	0.142945	0.141665	0.026036	0.00128	0.027316	0.024756

3.10 Thermodynamic properties

On the basis of Vibrational analysis at DFT/B3LYP/6-31G(d,p) and HF/6-31G(d,p) level, several thermodynamic parameters are calculated and are presented in Table 9. All the thermodynamic properties are helpful information for further study of the title molecule. This can be used to compute the other thermodynamic energies according to relationship of thermodynamic functions and estimate direction of chemical reactions according to second law of thermo dynamical field. The value of zero point vibrational energy (ZPVEs) in B3LYP/6-31G(d, p) is lower than HF/6-31G(d, p) method but the value of specific heat capacity(C) and entropy(S) are in B3LYP/6-31G(d, p) higher than HF/6-31G(d, p) method. Dipole moment reflects the molecular charge distribution and is given as vector in three dimensions.

Therefore, it can be used as descriptor to depict the charge movement across the molecule depends on the centre of positive and negative charges. The total dipole moment of the compound is calculated by B3LYP/6-31G(d, p) and HF/6-31G(d, p) methods are 1.8020 and 2.0284 Debye, respectively.

4. Conclusion

Density functional calculations have been successfully performed for the title compound. The stability of the molecule arising from hyper-conjugative interaction and charge delocalization has been analyzed using NBO analysis. In this compound, NBO analysis reveals that a strong intramolecular hyper conjugative interaction of π -electrons with the large energy contributions from π (C11-

C17) $\sigma^*(C2-C5)$ have energy value 21.55 kcal/mol. Electron donating from lone pair contribution LP(P1) to anti bonding $\sigma^*(C2-C5)$ $\sigma^*(C3-C6)$ $\sigma^*(C4-C7)$ is the most important interaction energy resulting stabilization of 3.18 kcal/mol and this interaction implies the existence of intramolecular transfer of energy between carbon atoms. The HOMO, LUMO and DOS analysis are used to determine the charge transfer within the molecule. HOMO-LUMO study reveals that HOMO-2 is localized on entire ring containing C3 and C4 atoms and partly on C2 except on P atom, whereas LUMO+2 is localized on the entire structure and partly on P atom. The MEP map indicates that, the weak negative regions are associated with C11-H26 and C13-H28 atoms and also the weak positive region on the hydrogen atoms. The Hirshfeld surface and fingerprint plot analysis, which act as a novel method of visualizing the intermolecular interactions, show that the close contacts of title molecule were dominated by C-C, H-P, P-H, H-C, C-H and H-H interactions. To investigate the stability of the compound, as seen from calculations that total energy obtained from PCM method decreases with the increasing polarity of the solvent and stability of the title compound increases from the gas-phase to solution-phase. The dipole moment, polarizability and hyperpolarizability values are predicted. The binding activity of the molecule with biological targets of interest was examined by docking analysis and discussed in terms of interaction energy calculated. The Fukui functions showed that the ring and substitution atoms are the most probable sites for electrophilic and nucleophilic attacks. Our density functional calculations of the compound and the calculated results will be helpful for the design and synthesis of new materials.

Table. 9. Thermodynamic parameters of Triphenylphosphine

THERMODYNAMIC PARAMETERS	DFT/B3LYP/6-31G(d,p)	HF / 6-31G (d,p)
SCF energy (a.u.)	-1036.11018	-1030.8103
Total energy Etotal ((Kcal/mol))	183.650	195.777
Vibrational energy (kcal/mol)	181.872	193.999
Zero point Vibrational energy (kcal/mol)	173.77112	186.63886
Specific heat, Cv (cal/mol K)	61.468	55.810
Entropy, S (cal/mol K)	132.640	127.846
Rotational constant (GHz)		
X	0.3787481	0.34689
Y	0.3486313	0.34685
Z	0.2144969	0.20590
Dipole moment μ (Debye)		
μ_x	0.0986	0.0975
μ_y	-0.1730	-0.1440
μ_z	1.7909	2.0210
Total	1.8020	2.0284

References

- [1] Haav; Kristjan, Saame, Jaan, Kütt, Agnes, Leito and Ivo, "Basicity of Phosphanes and Diphosphanes in Acetonitrile", European Journal of Organic Chemistry. 11, pp.2167–2172, 2012.
- [2] M Warchol, E. N Dicarolo, C. A Maryanoff and K. Mislow, "Evidence for the Contribution of the Lone Pair to the Molecular Dipole Moment of Triarylphosphines", Tetrahedron Letters, 16, pp.917–920, 1975.
- [3] D. E. C. Corbridge, "Phosphorus: An Outline of its Chemistry, Biochemistry and Technology (5th ed.)". Amsterdam: Elsevier. ISBN 0-444-89307-5.
- [4] H.Kooijman, A. L.Spek, K. J. C.; van Bommel, W. Verboom and D. N. Reinhoudt, "A Triclinic Modification of Triphenylphosphine", Acta Crystallographica, C54, pp.1695–1698, 1998.
- [5] B. J. Dunne and A. G. Orpen, "Triphenylphosphine: a Redetermination", Acta Crystallographica, C47: 345–347, 1991.
- [6] J. E.Cobb, C. M.Cribbs, B. R.Henke, D. E.Uehling, A. G.Hernan, C. Martin and C. M.Rayner, "Triphenylphosphine. In L. Paquette (ed.). Encyclopedia of Reagents for Organic Synthesis, New York: J. Wiley & Sons. 2004.
- [7] W.Kohn, and L. J. Sham, "Self-consistent equations including exchange and correlation effects", Physical Review, 140, pp.A1133–A1138, 1965.
- [8] A.D.Becke, "Density –functional thermochemistry.III. The role of exact exchange", J.Chem. Phys. 98, pp.5648–5652, 1993.
- [9] C.Lee, W.Yang and R.G.Parr, "Development of the Colle-Salvetti correlation-energy formula into a functional of the electron density", Phys. Rev. B 37, pp.785–789, 1988.
- [10] M. J.Frisch, G. W.Trucks, H. B.Schlegel et al., Gaussian 03, Revision A.1, Gaussian, Pittsburgh, Pa, USA, 2003.
- [11] A.Frisch, A.B.Nielsen and A.J.Holder 2007 Gaussview Users Manual, Gaussian Inc., Pittsburgh, 2007.
- [12] E.Scrocco and J. Tomasi, "Electronic Molecular Structure, reactivity and Intermolecular Forces; An Euristic Interpretation by Means of Electrostatic Molecular Potentials", Advances in Quantum Chemistry, 11, pp.115–193, 1978.
- [13] C.James, A.AmalRaj, Regunathan, I.H.Joe and V.S. Vayakumar, "Structural Conformation and Vibrational Spectroscopic Studies I. of 2,6-bis(p-N,N-dimethyl benzylidene) cyclohexane using density functional theory" J,Raman Spec. 12, pp.1381-1392, 2006.
- [14] A.R Krishnan, H.Saleem, S.Suashandrabose, N.Sundaraganesan and S.Sebastian, "Molecular structure, vibrational spectroscopic (FT-IR, FT-Raman), UV and NBO analysis of 2-chlorobenzonitrile by density functional method", Spectrochim.Acta, A78, pp.582-589, 2011.
- [15] EtemKose and AhmetAtac, "Synthesis, spectroscopic characterization and quantum chemical computations studies of (S)-N-benzyl-1-phenyl-5-(pyridin-2-yl)-pent-4-yn-2-amine", Spectrochim.Acta 97, pp.435-448, 2012.
- [16] E.Kavitha, N Sundaraganesan, and S.Sebastian, "Molecular Structure, Vibrational Spectroscopic and HOMO-LUMO studies of 4-nitroaniline by density functional method", Ind.J.Pure & Appl.Phys., 48, pp.20-30, 2010.
- [17] P. Politzer, M. C.Concha, and J. S.Murray, "Density functional study of dimers of dimethylnitramine", Int. J. Quantum Chem., 80, pp.184-192. 2000.
- [18] S. K.Wolff, D. J.Grimwood, J. J.McKinnon, M.J.Turner, D.Jayatilaka and M. A.Spackman, Crystal Explorer Version 3.1 2013.
- [19] S. K. Seth, N. C. Saha, S.Ghosh, and T.Kar, "Structural elucidation and electronic properties of two pyrazole derivatives: A combined X-ray, Hirshfeld surface analyses and quantum mechanical study", Chem. Phys. Lett. 506 pp.309-314, 2011.
- [20] Khaoula Azouzi, Besma Hamdi, Ridha Zouari and Abdelhamid Ben Salah, "Synthesis, structure and Hirshfeld

surface analysis, Vibrational and DFT investigation of (4-pyridine carboxylic acid) tetrachlorocuprate (II) monohydrate", *Bull. Mater.Sci.*, 40, pp.289–299, 2017.

[21] C.Sangeetha, R.Madivananeand V.Pouchaname, "Investigation of FT-IR, FT- Raman, UV-Visible, FT-NMR Spectra and Quantum Chemical Computations of Diphenylacetylene Molecule", *International Journal of Chemical and Physical Sciences*, 2, pp.12-28.2015.

[22] P.Geerlings, F.De Proft, andW.Langenaeker, "Conceptual Density Functional theory",*Chem. Rev.*, 103, pp.1793-1874, 2003.

[23] R. Pearson, "Recent advances in the concept of hard and soft acids and bases", *Chem. Ed.* 64, pp.561-567, 1987.

[24] R. G.Parr and P. K. Chattaraj, "Principle of maximum hardness", *J. Am. Chem. Soc.* 113, pp.1854-1855, 1991.

[25] T.Koopmans, "Ordering of wave functions and eigenvalues to the individual electrons of an atom", *Physica*, 1, pp.104-113, 1934.

[26] R.S.Mulliken,"A New Electro affinity Scale; Together with Data on Valence States and on Valence Ionization Potentials and Electron Affinities", *Journal of Chemical Physics*, 2, pp.782-795, 1934.

[27] V.Balachandran, S.Lalitha, S.Rajeswari, andV.K..Rastogi, "Theoretical investigation on the molecular structure, vibrational spectra, thermodynamics, HOMO-LUMO, NBO analyses and paramagnetic susceptibility properties of p-(p- hydroxyphenoxy)benzoic acid", *SpectrochimicaActa*, 121,pp.575-585,2014.

[28] Z.Zhou andH.V.Navangul, "Absolute hardness and aromaticity: MNDO study of . benzenoid hydrocarbons". *J. Phys. Org. Chem.*, 3, pp.784-788,1990.

[29] Y.X. Sun, Q.L..Hao, W.X.Wei, Z.X..Yu, L.D. Lu, X. Wang.andY.S.Wang. "Experimental and density functional studies on 4- (3,4dihydroxybenzylideneamino) antipyrine, and 4-(2,3,4-trihydroxybenzylideneamino)antipyrine", *J. Mol. Struct. THEOCHEM*, 904, pp.74-82,2009.

[30] R. Zhang, B. Du, G.Sun, and Y.X. Sun, "Experimental and theoretical studies on o-, m- and p- chlorobenzylideneaminoantipyrines", *Spectrochim. Acta* , 75, pp.1115-1124, 2010.

[31] TaharAbbaz; AmelBendjeddouand Didier Villemin; "Molecular orbital studies (hardness, chemical potential, electro negativity and electrophilicity) of TTFs conjugated between 1, 3-dithiole",. *International Journal of Advanced Research in Science, Engineering and Technology* 5, pp.5150-5161, 2018.

[32] Y.X.Sun, Q.L.Hao, W.X.Wei, Z.X.Yu, L.D.Lu, and X. Wang "Experimental and density functional studies on 4-(4-cyanobenzylideneamino)antipyrine", *Mol. Phys.*, pp.107, 223-235, 2009.

[33] O.Trott, and A. J.Olson, "AutoDockVina: Improving the speed and accuracy of docking with a new scoring function, efficient optimization and multithreading", *J. Comput. Chem.*, 31, pp.455-461,2010.

[34]R.T.Ulahannan, C.Y.Panicker, H.T.Varghese, R. Musiol, J.Josef, C. Van Alsenoy, J.A.War andS.K.Srivastava, "Molecular Structure, FT-IR, FT-Raman, NBO, HOMO and LUMO, MEP, NLO and molecular docking study of 2-[(E)-2-(2-bromophenyl)- ethenyl]quinoline-6-carboxylic acid", *Spectrochim. Acta* 151, pp.184-197, 2015.

[35]B. Sureshkumar, Y.Sheena Mary, C.YohannanPanicker, S. Suma, J.StevanArmaković, C. Sanja. Armaković, Van Alsenoy and B. Narayana, "Quinoline derivatives as possible lead compounds for anti-malarial drugs: spectroscopic, DFT and MD study", *Arabian Journal of Chemistry*, 13, pp.632-648. 2020.

[36]M. Kavimani , V. Balachandran ., B.Narayanaand K.. Vanasundari, "Conformational stability, spectroscopic (FT-IR, FT-Raman) analysis, fukui function, Hirshfeld surface and docking analysis of Naphthalene-2-lyoxy acetic acid by density functional theory", *International Journal of Pure and Applied Researches*, 1, pp.7-14.2017.

[37]N.Benhalima, S.Yahiaoui, N.Boubegra, M.Boulakoud, et.al, "Quantum chemical investigation of spectroscopic, electronic and NLO properties of (1E,\$E)-1-(3-nitrophenyl)-5-phenylpenta-1,4-dien-3-one", *International Journal of Advanced Chemistry*, 6, pp.121-131.2018.

[38]P.W.Ayers.and R.G. Parr, "Variational Principles for describing Chemical reactions: The Fukui Function and Chemical Hardness Revisited", *J.Am.Chem.Soc.*,122, pp. 2010-2018. 2000.

[39]R.G.Parr and W. Uang, "Density functional approach to the frontier-electron theory of chemical reactivity",*J.Am.Chem.Soc.*,106, pp.4049-4050, 1984.

[40]P.K..Chattaraj, B. Maitiand. U. Sarkar, "Philicity: A Unified treatment of Chemical Reactivity and Selectivity", *J.Phys.Chem.A.*,107, pp.4973-4975, 2003.

[41]C.A Morell; AGrand and Toro-Labbe, "New Dual descriptor for Chemical reactivity", *J.Phys.Chem. A.*,109, pp.205-212, 2005.